

Modeling of Selective Area Laser Deposition Vapor Infiltration (SALDVI) of Silicon Carbide

K. Dai, J. Crocker, L. Shaw and H. Marcus

Department of Metallurgy and Materials Engineering
Institute of Materials Science
University of Connecticut, Storrs, CT 06269

ABSTRACT

Selective Area Laser Deposition Vapor Infiltration (SALDVI) is a developing solid freeform fabrication (SFF) technique in which porous layers of powder are densified by infiltrating the pore spaces with solid material deposited from a gas precursor during laser heating. A 3D finite element model was developed that simulates SALDVI of silicon carbide. The model predicts the laser input power and the distribution of vapor deposited SiC within the powder bed as well as on the surface of the powder bed (SALD). The model considers a moving Gaussian distribution laser beam, temperature- and porous-dependent thermal conductivity, specific heat and temperature-dependent deposition rate. Furthermore, the model also includes closed-loop control of the laser power to achieve a desired target processing temperature on the top surface of the powder bed. The simulation results agree fairly well with experimental data for simple geometries and offer guidelines for further experimental studies of the SALDVI process.

Keywords: Finite element modeling, Silicon carbide, Solid freeform fabrication, Selective Area Laser Deposition Vapor Infiltration.

INTRODUCTION

Chemical vapor infiltration (CVI) is a promising process where a vapor-phase precursor is transported into the porous preform, and a combination of gas and surface reactions leads to the deposition of the solid matrix phase and densifies the part. Selective Area Laser Deposition Vapor Infiltration (SALDVI) process which combines the Selective Area Laser Deposition (SALD) process and the CVI process is a developing solid freeform fabrication (SFF) technique aimed at the direct fabrication of ceramic and ceramic/metal structures and composites. SALDVI experiments have shown that the size and geometry of the densified part depend in large part on the temperature distribution in the SALDVI workpiece among other parameters [1]. The understanding of the temperature distribution in the SALDVI process is very important to achieve the insight into the effect of various process parameters on the shape of the SALDVI workpiece. During the SALDVI process the relative density of the workpiece continuously changes with processing time until it reaches near full density. Because of such continuous changes in the relative density and thus the continuous change in thermal conductivity of

the SALDVI workpiece, the transient temperature field of the SALDVI workpiece is too complex to calculate by analytical methods. The development of finite element modeling (FEM) has offered opportunities to solve it. Many efforts of numerical modeling have been carried out to investigate the effect of various processing parameters on the SALD process. However, the SALDVI process has its specific features compared with the general SALD process. The present study provides 3-dimensional thermal analyses of the SALDVI process. It will provide guidance for intelligent selection of various parameters and help to understand other SFF processes involving powder-to-dense-body transition such as selective laser sintering (SLS).

MODEL DESCRIPTION

The goal of this modeling effort is to simulate the SALDVI process in which a porous powder bed is locally densified by laser chemical vapor infiltration. The effect of the laser processing conditions on the size, geometry, and densification history of the workpiece during processing is evaluated. The finite element model used for this purpose is shown in Figure 1 and calculated using the ANSYS 3-dimensional thermal conductive element (Solid70). This model is used to calculate the temperature distribution in the powder bed due to laser heating. The local Chemical Vapor Deposition (CVD) growth rate in the powder bed is calculated from the local temperature and the resulting change in powder bed density is determined. The density-dependent physical properties of the workpiece are updated and are used to calculate the new temperature distribution. In this step-wise manner, the evolution of densification by the Laser Chemical Vapor Infiltration (LCVI) is modeled. The powder bed before densification is assumed to have a dimension of 14-mm length ($L=14\text{mm}$), 4-mm width ($W=4\text{mm}$) and 1.2-mm height ($H=1.2\text{mm}$). Thus, the powder bed in this study is very thick in comparison with the layer-by-layer fabrication technique, which typically has a powder layer thickness less than 0.5 mm. However, the present simulation allows for assessment of building the first solid layer from a thick powder bed rather than from a thin powder layer on the top of a solid substrate or a previously densified layer. Densification of thin powder layer will be modeled in the future effort.

As shown in Figure 1, the SALDVI process is modeled by scanning a laser beam along the surface of a powder bed at a uniform velocity and calculating the resulting temperature distribution. In this model the laser beam is modeled as a heat flux with a Gaussian power distribution as an incoming heat source.

In SALDVI experiments, an optical pyrometer is used to continually monitor the temperature distribution at the surface of the powder bed during laser heating. This pyrometer temperature is used as the feedback parameter in a closed-loop control program that adjusts the incident laser power as needed to achieve a desired constant pyrometer temperature. In the simulation, in order to simulate the closed loop control program used in the experiments, the laser power is modified from one time step to the next if the pyrometer simulation temperature differs from the desired target temperature. This step can make the temperature read by pyrometer approach the desired target surface temperature in the simulation.

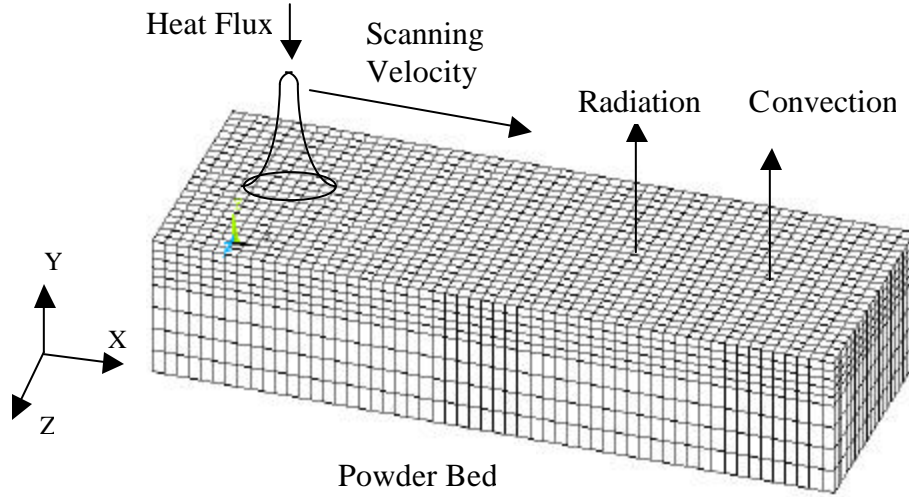


Figure 1. Finite element model of the SALDVI process.

The thermal conductivity, K_T [W/MM-K], is a thermal and solid fraction dependent parameter that is given by equations (1) and (2)

For 42 % dense 15 μ m diameter SiC powder [2]:

$$K_T = 3.127 * 10^{-5} T^{0.34196} (1 - P_n) / 0.42 \quad \text{when } 1 - P_n \leq 0.42 \quad (1)$$

and when sufficient CVI has occurred forming a continuous solid network, there are a upper bound K_{TH} and a lower bound K_{TL} [2-3]

$$K_{TH} = 12.709 T^{-0.89464} (1 - P_n)^{1.5} \quad (2a)$$

$$K_{TL} = 24.7 T^{-1.1896} (1 - P_n)^{1.5} \quad (2b)$$

In this model, the effective thermal conductivity K_T is taken between the upper bound and the lower bound.

$$K_T = 0.2 K_{TH} + 0.8 K_{TL} \quad \text{when } 1 - P_n > 0.42 \quad (2c)$$

where P_n is the porous fraction at step n, and T is the temperature at step n.

The specific heat is given by [4]

$$C_p = (1 - P_n) 90.14428 T^{0.37511} \text{ [J/Kg.K]} \quad (3)$$

SIMULATION RESULTS AND THE COMPARISON WITH EXPERIMENTS

In experiments, a porous SiC powder bed with an initial solid fraction of 0.42 and 15 μ m average particle diameter is locally densified by laser chemical vapor infiltration

with 10 Torr Si(CH₃)₄ gas at three different laser scanning speeds. The CO₂ laser beam is focused to a diameter of 1 mm and the laser power is continuously adjusted to obtain a surface temperature of 1000°C measured by the pyrometer. The experimental conditions of the three cases that will be simulated in this work are shown in Table 1.

Figure 2 shows the simulation value of pyrometer temperature during the scanning process. The bias is less than 2% of the desired pyrometer temperature, which shows that the closed-loop temperature control in experiment can be adequately simulated in this model. Figure 3 shows the instantaneous temperature distributions in the powder bed for the three scan speeds after the beam has scanned a distance of 12.25 mm. We can see from this figure that the temperature gradient becomes higher with the faster scanning rate.

Table 1. Experimental cases to be simulated

Desired Pyrometer Temperature (K)	Scanning Speed (μm/s)	Powder Packing Fraction	Initial Particle Radius (μm)
1273	1.25, 2.50 and 5.0	0.42	7.5

Figure 4 shows the laser input power history needed to obtain the desired pyrometer surface temperature of 1000°C in the experiment and simulation. Figure 5 shows the distribution of solid material (powder and vapor deposition) in the powder bed after scanning process in the experiment and simulation. All the three different scanning rate cases indicate that a good agreement exists between the experimental and simulation results. From these two figures we can see that as the laser scanning rate decreases, the incident laser power and the infiltration of SiC into the powder bed will increase. As the workpiece becomes denser and larger in size with lower scanning rates, the higher the effective thermal conductivity and the more readily the heat dissipates from the process zone. This is illustrated in Figure 3 where the overall size of the heated zone in the powder bed becomes larger as the scanning rate decreases while the high temperature region (1423 K isotherm) becomes smaller.

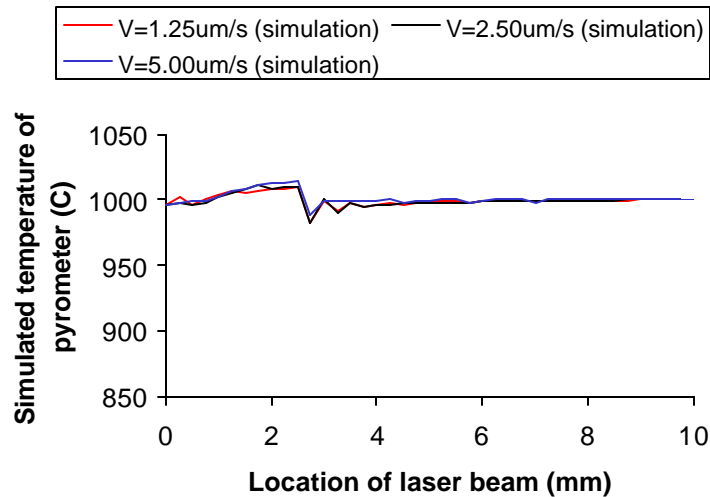


Figure 2. The simulated temperature value of pyrometer during the scanning process

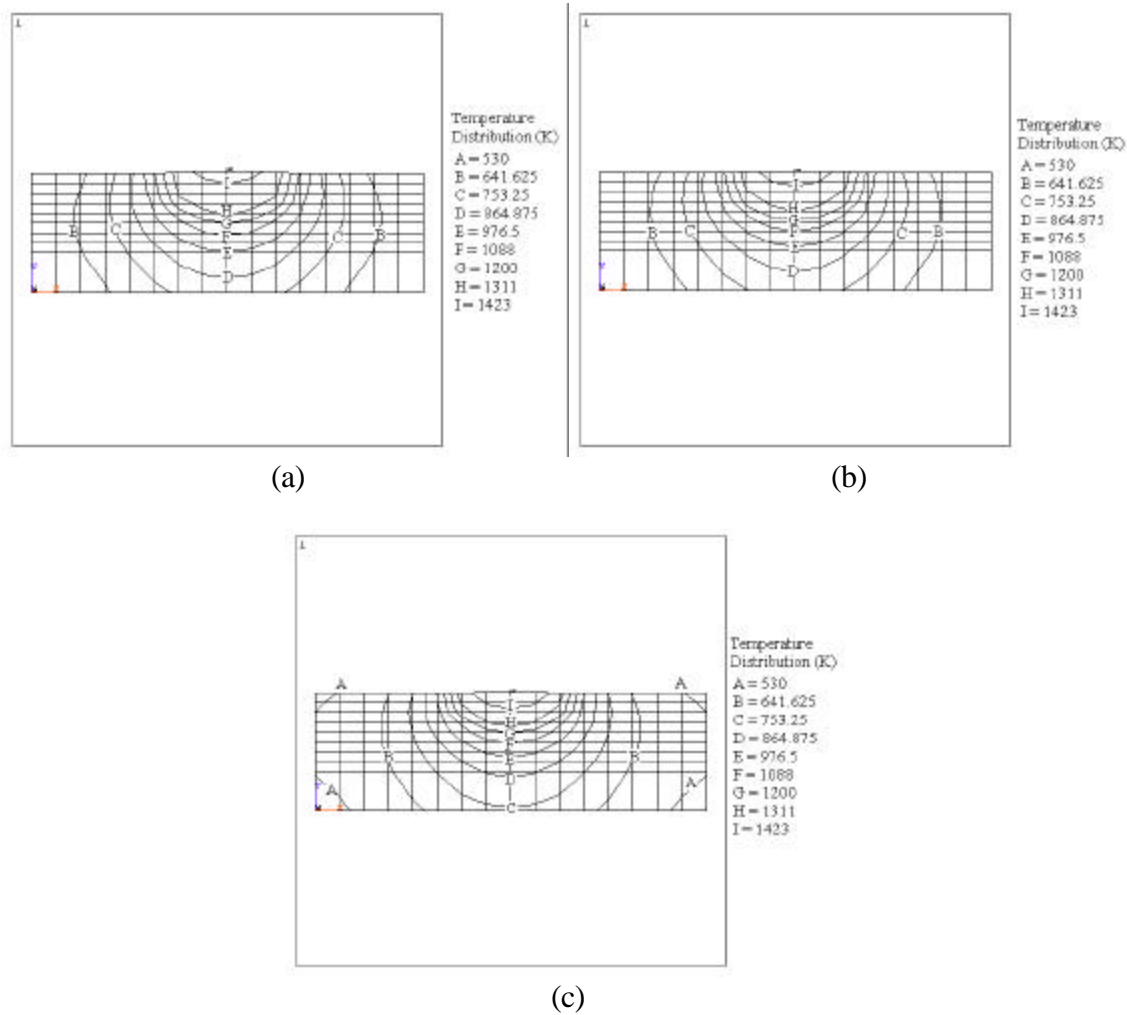


Figure 3. Temperature distribution in the powder bed at the cross section of $X = 12.25$ mm and scanning rate of (a) $1.25 \mu\text{m/s}$, (b) $2.50 \mu\text{m/s}$, and (c) $5.00 \mu\text{m/s}$.

Comparing Figures 2 and 4, we also can see that uniform temperature on the top surface of powder bed during laser scanning process needs non-uniform laser power at the initial scanning period and nearly uniform laser power beyond this initial period. The reason is that at the beginning of the laser scanning, the laser-heated area is surrounded by powder with a much lower thermal conductivity and heat dissipation is slow. Thus, less laser incident power is needed to heat the powder under the laser beam to the desired pyrometer surface temperature. As the scanning proceeds, the part density and size increases and more heat is dissipated through thermal conduction along the previously densified section with a higher effective thermal conductivity. Thus, the laser incident power will increase with the moving of the laser beam. Finally, a steady state is reached that heat conduction through the previously densified section does not change much with time and the laser incident power reaches a nearly uniform value. Since more heat is conducted away through the previously densified section in the steady state region than

that in the initial transient region, the laser incident power in the steady state region is larger than that in the initial transient region.

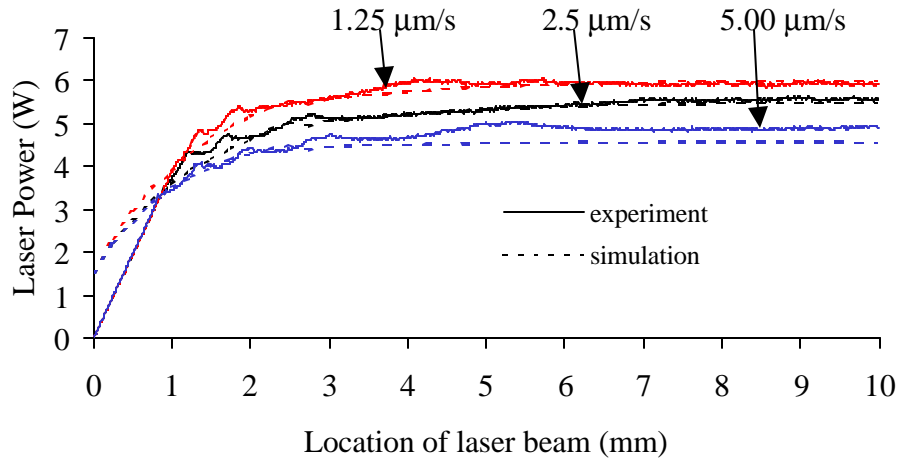


Figure 4. Comparison between the experimental and simulated incident laser power during the scanning process.

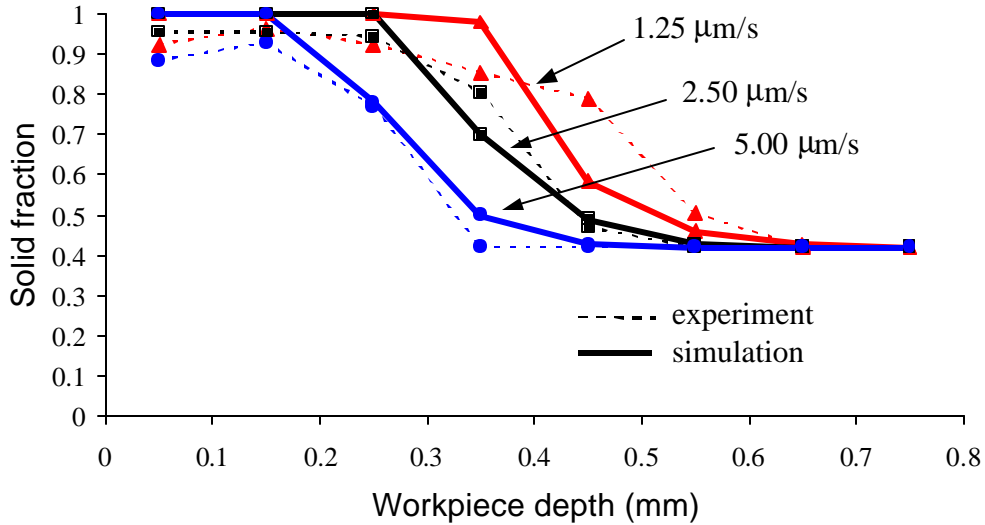


Figure 5. Comparison between the experimental and simulated solid fraction distribution in depth direction under the center of the laser beam after the scanning process at $x=7$ mm.

The distribution of vapor deposited SiC on the surface of the powder bed (SALD) on the transversal section with different laser scanning rate can be observed in Figure 6. The SALD increases as the laser scanning rate decreases due to the faster scanning rate having less time for SiC to deposit on the surface of powder bed. The height of the SALD is larger at the center region due to the Gaussian power distribution of the incident laser beam. Due to the small SALD ($<40\mu\text{m}$) when scanning rates are $2.50\mu\text{m/s}$ and

5.00 $\mu\text{m/s}$, the SALD is hardly to measure. In figure 6, only the SALD with scanning rate 1.25 $\mu\text{m/s}$ is measured. The trends between simulation and measurement are consistent.

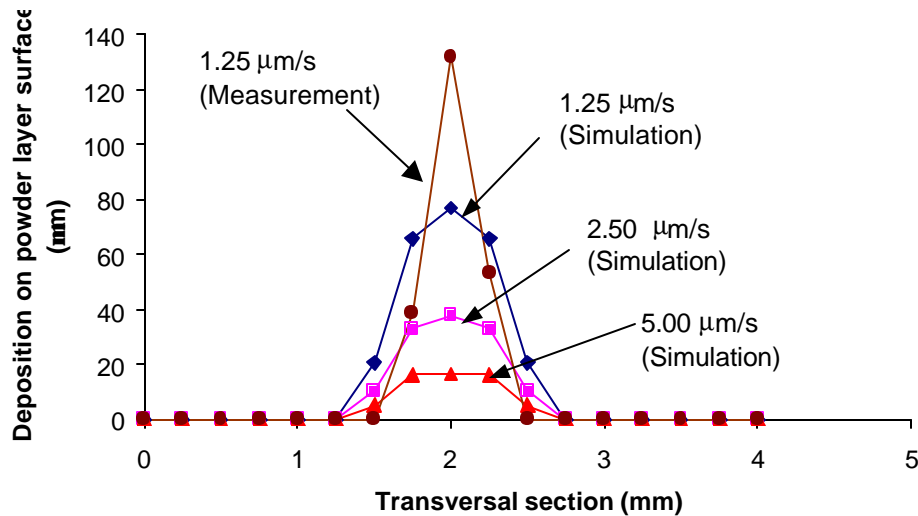


Figure 6. Simulation results of the distribution of vapor deposited SiC on the surface of the powder bed (SALD).

CONCLUSIONS

- 1) The simulation results of the incident laser power history and the distribution of vapor infiltrated SiC in the powder bed agree fairly well with the experiments.
- 2) As the laser scanning rate decreases, the incident laser power will increase, the deposition of SiC both within the powder bed as well as on the surface of the powder bed (SALD) will increase.
- 3) Uniform temperature on the top surface of powder bed during laser scanning process needs non-uniform laser power at the initial scanning period and nearly uniform laser power elsewhere.

Acknowledgements – The authors gratefully acknowledge financial support provided by the National Science Foundation under Grant No: DMI-9908249 and the Office of Naval Research under Grant No: N00014-95-1-0978.

REFERENCES

1. J.E. Crocker, L. Sun, H. Ansquer, L. Shaw, and H.L. Marcus, Processing and Characterization of SALDVI Ceramic Structures, Proceedings of the Solid Freeform Fabrication Symposium, David L. Bourell et al. (eds), The University of Texas at Austin, 495-501:1999.

2. Y.S. Touloukian, R.W. Powell, C.Y. Ho, and P.G. Clemens, Thermophysical Properties of Matter, Volume 2, THERMAL CONDUCTIVITY Nonmetallic Solids, IFI/Plenum, New York, New York, 1970.
3. E. Litovsky, M. Shapiro, and A. Shavit, Gas Pressure and Temperature Dependences of Thermal Conductivity of Porous Ceramic Materials: Part 2, Refractories and Ceramics with Porosity Exceeding 30 %, J. Am. Ceram. Soc., 1996, 79[5] 1366-76.
4. Y.S. Touloukian and E.H. Buyco (Editors), Thermophysical Properties of Matter, Volume 5, SPECIFIC HEAT: Nonmetallic Solids, IFI/Plenum, New York, New York, 1970.